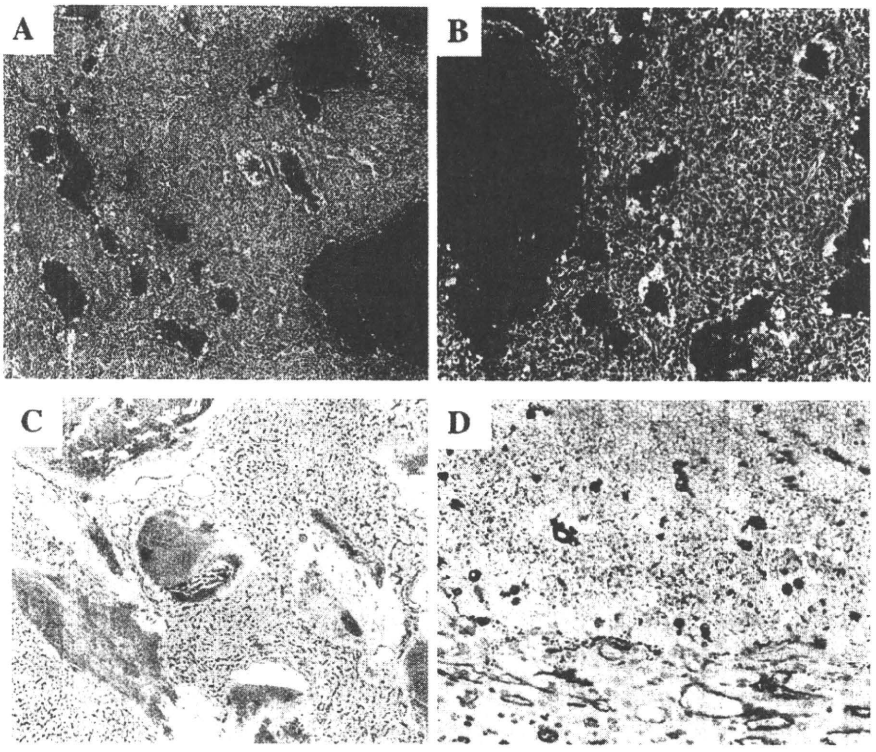

Figure 3. Histological features of peliotic changes. (A and B) Small and large blood lakes are observed in moderately differentiated HCC and irregular dilatation of sinusoid-like blood spaces of the tumor (H&E stain). (C and D) Immunostaining for CD34 shows no positive cells along the spaces of peliotic change.

or necrosis was not observed around peliotic changes. A varying degree of sinusoidal dilatation was observed around peliotic changes. In the control group, 116 tumors (66%) were moderately differentiated, 55 tumors (31%) were poorly or moderately to poorly differentiated and 6 tumors (3%) were well-differentiated. Among 111 PHCCs in which non-cancerous areas were examined, 66 cases (59%) were chronic hepatitis associated with varying degrees of fibrosis and 45 (41%) were liver cirrhosis. Among the 176 cases in the control group, 85 cases (48%) were chronic hepatitis and 91 (52%) cirrhosis. No significant difference was ntoed in the background liver between the groups.

Recurrence rate after resection. Follow-up data following surgery were obtained in 32 PHCC cases and in 39 controls. Follow-up periods ranged from 4 to 105 months (mean 38±25.7 SD). Recurrence occurred in 18 PHCC cases (56%) and in 17 controls (44%). There was no significant difference between the 2 groups.

Discussion

Peliotic changes are frequently observed in HCCs. However, the question raised is whether peliotic change is essentially different from hemorrhage of the tumor. In general, degenerative change and/or necrosis are observed around hemorrhage of HCC tumors. Put differently, degeneration and/or necrosis of tumor tissue cause hemorrhage in HCC. On the other hand, tumor tissues around peliotic changes are not degenerative or necrotic and blood is localized within the spaces. Thus, it is suggested that peliotic changes are different from hemorrhage. However, when peliotic changes become extensive, they may rupture and hemorrhage may develop.

Various factors are suggested in the pathogenesis of peliosis hepatis. These factors are excessive alcohol intake, hormonal agents such as oral contraceptives and anabolic steroids, as well as chronic wasting diseases, including malignant tumors and tuberculosis (8-12). It was also suggested that blood constituents infiltrate the Disse's spaces resulting in cyst-like change of the sinusoids following the mechanical disorder of the sinusoidal endothelial cells (13). In a study of 12 cases of peliosis hepatis, Zafrani *et al* suggested that the developmental mechanism of peliosis hepatis obstructed blood channels caused by sinusoidal destruction accompanying hepatocellular necrosis or the abnormal bonding of sinusoids and the central vein (2). Based on the fact that peliotic changes were frequently observed in the encapsulated tumors, the mechanism of peliotic change in HCC was explained by endothelial damage due to sinusoidal dilatation following increased intratumoral pressure. This assumption is supported by the fact that similar peliotic changes are frequently observed in liver cell adenoma, which is also an expansive tumor with frequent encapsulation. Sugimachi *et al* suggested a particular relationship between peliotic change in HCC and angiopoietin-2 (Ang-2), which play a regulatory role in tumor vessel remodeling (14).

No significant clinical differences were noted between the PHCC and control groups other than the significantly higher frequency of hyperechoic and/or mosaic patterns in PHCCs on ultrasonography. The most common histological feature reflecting hyperechogenecity in HCC is fatty change of the tumor which most frequently occurs in small well-differentiated tumors up to ~2 cm in diameter (15). HCC tumors with

hyperechoic and/or mosaic patterns among tumors >3-4 cm in diameter are rarely found. In the present study, these tumors proved to be PHCCs.

Although peliotic change in HCC has little clinical significance, it is necessary for clinicians and pathologists to distinguish the presence of peliotic change as a morphological feature that modifies ultrasonographic patterns of HCC.

Acknowledgements

We thank Ms. Sachiyo Maeda and Ms. Misato Shiraishi for their technical assistance on immunohistochemical staining. This study was supported in part by the Sarah Cousins Memorial Fund, Boston, MA, USA.

References

1. Karasawa T, Shikata T and Roger DS: Peliosis hepatis: report of nine cases. Acta Pathol Jpn 29: 457-469, 1979.
2. Zafrani ES, Cazier A, Baudelot AM and Feldmann G: Ultrastructural lesions of the liver in human peliosis. A report of 12 cases. Am J Pathol 114: 349-359, 1984.
3. Asano S, Wakasa H, Kaise S, Nishimaki T and Kasukawa R: Peliosis hepatis: Report of two autopsy cases with a review of literature. Acta Pathol Jpn 32: 861-877, 1982.
4. Wagner E: Fall von Blutcysten der Leber (In German). Arch Heilk 2: 369-370, 1861.
5. Kojiro M: Peliosis hepatis (In Japanese). Acta Hepatol Jpn (KANZO) 38: 583-586, 1997.
6. Grazioli L, Morana G, Caudana R, *et al*: Hepatocellular carcinoma: correlation between gadobenate dimeglumine-enhanced MRI and pathological findings. Invest Radiol 35: 25-34, 2000.
7. Brancatelli G, Baron RL, Peterson MS and Marsh W: Helical CT screening for hepatocellular carcinoma in patient with cirrhosis: frequency and cases of false-positive interpretation. Am J Roentgenol 180: 1007-1014, 2003.
8. Loomus GN, Aneja P and Bota RA: A case of peliosis hepatis in association with tamoxifen therapy. Am J Clin Pathol 80: 881-882, 1983.
9. Dejgaard A, Krogsgaard K and Jacobsen M: Veno-occlusive disease and peliosis of the liver after thorotrast administration. Virchows Arch A Pathol Anat Histopathol 403: 87-94, 1984.
10. Czapar CA, Weldon-Linne CM, Moore DM and Rhone DP: Peliosis hepatis in the acquired immunodeficiency syndrome. Arch Pathol Lab Med 110: 611-613, 1986.
11. Russmann S, Zimmermann A, Krahenbuhl S, Kern B and Reichen J: Veno-occlusive disease, nodular regenerative hyperplasia and hepatocellular carcinoma after azathioprine treatment in a patient with uncreative colitis. Eur J Gastroenterol Hepatol 13: 287-290, 2001.
12. Drevelengas A, Chourmouzi D and Boulogianni G: Peliosis of the liver in a patient with prostate carcinoma. JBR-BTR 86: 158-159, 2003.
13. Shim SG, Paik SW, Hyun JG, *et al*: Lipiodol accumulation in focal peliosis hepatis with sinusoidal dilatation. J Clin Gastroenterol 32: 356-358, 2001.
14. Sugimachi K, Tanaka S, Taguchi K, Aishima S, Shimada M and Tsuneyoshi M: Angiopoietin switching regulates angiogenesis and progression of human hepatocellular carcinoma. J Clin Pathol 56: 854-860, 2003.
15. Kutami R, Nakashima Y, Nakashima O, Shiota K and Kojiro M: Pathomorphologic study on the mechanism of fatty change in small hepatocellular carcinoma of humans. J Hepatol 33: 282-289, 2000.

Hepatology Research 2010; **40**: 330–336 doi: 10.1111/j.1872-034X.2009.00604.x

Original Article

Accelerated expression of a Myc target gene *Mina53* in aggressive hepatocellular carcinoma

Sachiko Ogasawara,[1] Mina Komuta,[2] Osamu Nakashima,[1] Jun Akiba,[1] Makoto Tsuneoka[3] and Hirohisa Yano[1]

[1]*Department of Pathology, Kurume University School of medicine, Asahi-machi, Kurume, Fukuoka,* [2]*Department of Pathology, Keio University School of medicine, Shinano-machi, Shinjuku-ku, Tokyo, and* [3]*Faculty of Pharmacy, Takasaki University of Health and Welfare, Nakaorui-machi, Takasaki, Gunma, Japan*

Aim: Expressions of the *myc* target genes *Mina53* and *mimitin* are high in esophageal squamous cell carcinoma and colon cancer, and their relationship to cell proliferation and patient prognosis has been reported. Because *c-myc* gene expression is closely related to hepatocellular carcinoma (HCC) growth or formation and/or maintenance, we examined the *Mina53* and *mimitin* expressions in HCC.

Methods: Surgically resected 53 HCC tissues were immunohistochemically examined for *Mina53* and *mimitin* expressions and their relationship to clinicopathological factors.

Results: Diffuse *Mina53* expression was observed in the nuclei of cancer cells in the tumor nodule, but was often strong at the periphery of tumor nodules. Diffuse or scattered expression of *mimitin* was observed in the cytoplasm of HCC cells in tumor nodules. *Mina53* expression was higher in poorly differentiated HCC than in well-differentiated HCC, and significant relationship to histological grade was observed. The cases with a high *Mina53* expression also had a high expression of a proliferation marker MIB-1. This suggested the involvement of *Mina53* in cell proliferation. *Mina53* expression was high in the tumors of >2 cm of diameter than in ≤2 cm ($P < 0.01$). *Mimitin* expression tended to be high in tumors of >2 cm, but no significant relationship was observed either to histological grade, MIB-1 expression, or the other clinicopathologic factors.

Conclusions: Our findings suggested that *Mina53* expression is accelerated in HCC with a lower histological grade, with cell proliferation capability, or with a larger diameter, and *Mina53* is related to biological malignancy of HCC.

Key words: hepatocellular carcinoma (HCC), MIB-1 index, *mimitin*, *Mina53*

INTRODUCTION

HEPATOCELLULAR CARCINOMA (HCC) is one of the most common cancers worldwide and a leading cause of cancer mortality, especially in countries with a high prevalence of chronic infections with hepatitis B virus (HBV) and hepatitis C virus (HCV). The biological significance of some proto-oncogenes, tumor suppressor genes, growth factor genes and virologic factors has been implicated in hepatocarcinogenesis.[1,2] The mechanism of hepatocarcinogenesis is thought to be multifactorial that involves multiple oncogenes.[3]

Correspondence: Dr Sachiko Ogasawara, Department of Pathology, Kurume University School of Medicine, 67 Asahi-machi, Kurume, Fukuoka 830-0011, Japan. Email: sachiko@med.kurume-u.ac.jp
Received 18 May 2009; revision 21 August 2009; accepted 26 August 2009.

The *myc* family of proto-oncogenes consists mainly of 3 genes, i.e. *c-myc*, N-*myc* and L-*myc*.[4–7] Deregulated expression of *myc* family genes has been noted in many neoplastic diseases in a wide range of vertebrates including humans.[6,7] The *myc* family genes also relate to many biological phenomena besides tumorigenesis, and the genes control apoptosis and cell differentiation in addition to cell proliferation.[8,9]

c-myc is one of the most widely studied proto-oncogenes, and it is the best-characterized member in the *myc* gene-family. Generally, *c-myc* expression is associated with cell proliferation and it is down-regulated in quiescent and differentiated cells.

Recently, Tsuneoka *et al.* identified the novel genes, *Mina53* (*myc*-induced nuclear antigen)[10] and *mimitin* (*myc*-induced mitochondria protein),[11] and presented that *c-myc* directly induced their expressions. The *Mina53* gene encodes a protein with a molecular weight of 53 kDa that is localized in nucleus and with part of

the protein concentrated in the nucleolus. The *mimitin* gene encodes a protein with a molecular weight of 20 kDa that is localized in mitochondria. *Mina53* expression was reported in esophageal squamous cell carcinoma (ESCC)[12] and colon cancer,[13] the expression was high in poor prognostic cases of ESCC, and its relationship to cell proliferation has been indicated. *Mimitin* expression was also reported in ESCC, and its relationship to cell proliferation was shown.[11] However, their functions are not yet fully clarified, and there have been no studies on them in the tissues level of hepatocytes. Because *c-myc* gene expression is closely related to HCC growth or formation and/or maintenance,[14–16] we examined the relationship between *Mina53* and *mimitin* expressions in HCC tissues and clinicopathological factors.

MATERIALS AND METHODS

TISSUE SAMPLES OF HCC and non-HCC were obtained from 53 patients who underwent surgical resection of tumors in the Kurume University Hospital and its affiliated hospitals in the period between 1994 and 1996. Before the surgery, none of these patients had received any form of treatment such as arterial embolization and chemotherapy. Histologically, the 53 surgically obtained samples consisted of 6 well+moderately differentiated HCCs, 35 moderately differentiated HCCs, 9 moderately+poorly differentiated HCCs and 3 poorly differentiated HCCs. Non-cancerous area presented liver cirrhosis ($n = 23$) or chronic hepatitis ($n = 30$).

The HCC specimens were immunohistochemically stained and examined for the relationship between the expressions of *Mina53* or *mimitin* and such clinicopathologic factors as histological grade of HCC, capsule formation, capsule infiltration, tubular invasion, recurrence rate, survival rate, and histological change in non-HCC tissues (normal, hepatitis, liver cirrhosis).

For immunohistochemical examinations, the surgically obtained tissue samples were formalin fixed and paraffine embedded by using the usual procedure. Serial sections 4-μm thick were mounted on coated slides and deparaffinized in xylene and graded alcohol. The sections were soaked in Target Retrieval Solution (Dako, Carpinteria, CA), and treated in a microwave oven for 30 min. Mouse monoclonal anti-*Mina53* antibody (concentration: 3.4 μg/mL) and rabbit polyclonal anti-*mimitin* antibody (concentration: 0.7 μg/mL) were established at Division of Human Genetic Department of Forensic Medicine, Kurume University School of Medicine and specificity of these antibodies was confirmed in previous studies.[10,11] Ki-67 antibody (clone MIB-1, concentration: 0.8 μg/mL) was obtained from Dako A/S (Glostrup). The sections were incubated with primary antibodies for 60 min at room temperature. Immunohistochemical staining was performed using CSA II (Dako) according to the manufacturer's protocol. The peroxidase reaction was developed with the substrate 3,3-diaminobenzidine and H_2O_2. After light counterstaining with hematoxylin, the slides were dehydrated, coverslipped, and observed under a microscope.

By examining the cancerous tissues, the specimens were classified into 3 groups according to the percentage of HCC cells that were immunohistochemically positive to *Mina53* and *mimitin*, i.e. negative (–) if 0%, low-expression (+) if 1–33%, high-expression (++) if 34%<.

The Ki-67 staining results (MIB-1 index) of tumor cells were evaluated in the following manner: In the *Mina53*- or *mimitin*-positive samples, MIB-1 index in the area that contained *Mina53*- or *mimitin*-positive cells and presented the highest MIB-1 expression level was evaluated. In the *Mina53*- or *mimitin*-negative samples, MIB-1 index in the area with the highest MIB-1 expression level was evaluated. Total number of stained cells was estimated as the sum of positive and negative tumor cells, and then the ratio of positive cell number to the estimated total cell number was obtained. The average MIB-1 index in our specimens was 28.2%, and the specimens were classified into two groups (≤28% and 28%<).

Statistics

The Mann–Whitney *U*-test was used to examine the relationship between known prognostic factors and the expression level of *Mina53* or of *mimitin*, and MIB-1 index. The Kaplan–Meier method was used to calculate disease-free survival rate. All statistical analyses were performed with StatMate III (ATMS, Tokyo). *P*-values less than 0.05 were considered statistically significant.

RESULTS

Immunohistochemistry

MINA53 EXPRESSION WAS detected in the nuclei of HCC cells in tumor nodule and in portal vein tumor thrombi. The expression was observed diffusely in tumor nodules, but it was often strong HCC cells at the periphery of tumor nodules (Fig. 1a,b). The expression was also observed in lymphocytes infiltrating into the capsules (data not shown). In non-cancerous tissues,

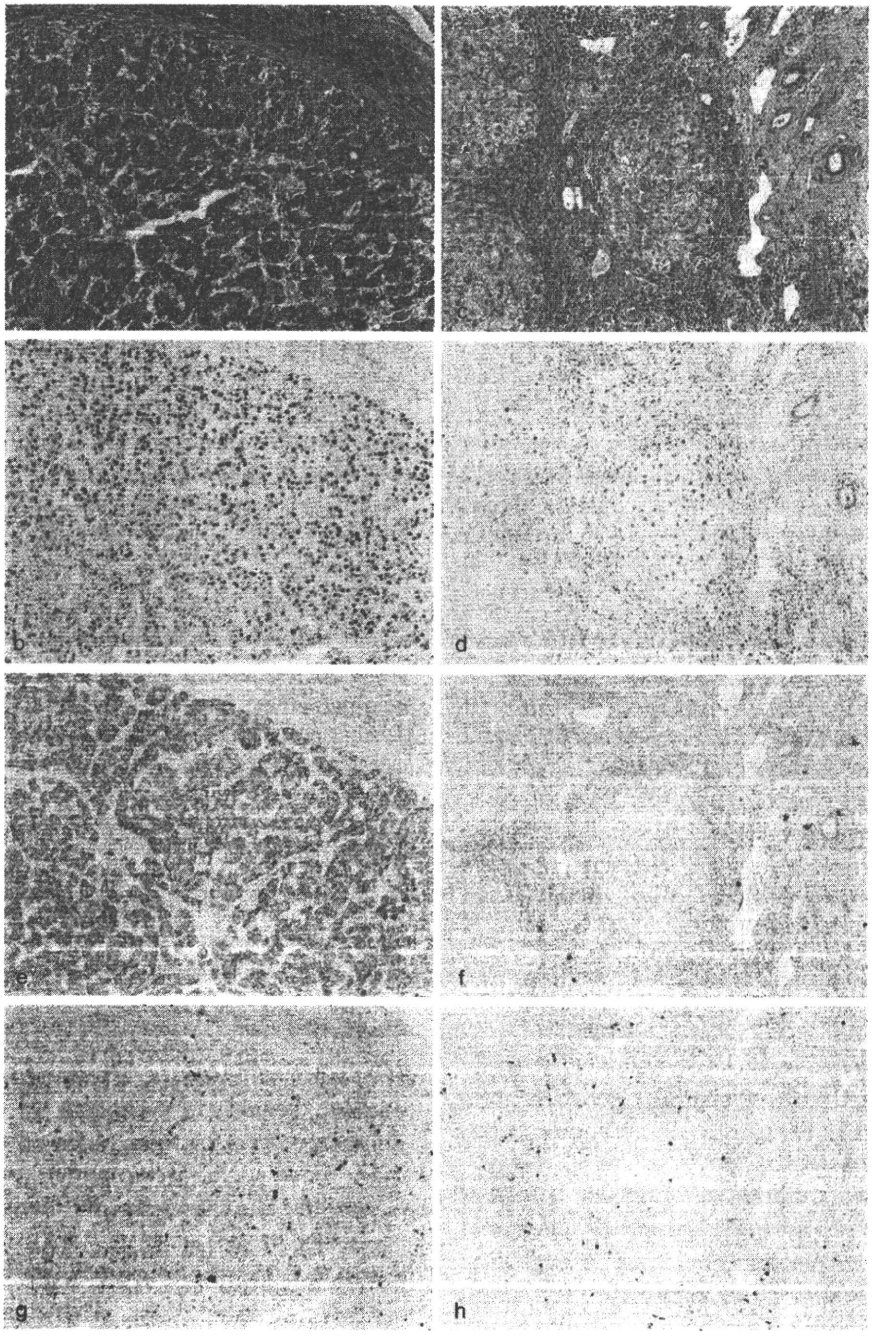

Figure 1 Immunohistochemical staining of *Mina53*, *mimitin* and MIB-1 in hepatocellular carcinoma (HCC) and non-cancerous tissues. (a) Moderately differentiated HCC (hematoxylin & eosin staining, ×100). (b) *Mina53* expression in the nuclei of cancer cells. HCC cells at the periphery of tumor nodule show stronger expression (×100). (c) Non-cancerous area (hematoxylin & eosin staining, ×100). (d) *Mina53* expression was observed in the nuclei of bile duct epithelium, of some of the lymphocytes in a portal area, and of hepatocytes around portal areas (×100). (e) Diffuse *mimitin* expression in the cytoplasm of HCC cells (×100). (f) *Mimitin* expression in bile duct epithelium and some cells in portal areas (×100). (g) MIB-1 expression in the nuclei of cancer cells of tumor nodule (×100). (h) MIB-1 expression in non-HCC tissue (×100).

Table 1 Relationship between clinicopathological factors and *Mina53* expression in hepatocellular carcinoma ($n = 53$)

Mina53 expression level		–	+	++
Histological grade*:				
Well+moderately differentiated		3	3	0
Moderately differentiated		8	12	15
Moderately+poorly differentiated		0	2	7
Poorly differentiated		0	1	2
MIB-1 index (%)**:	≤28	11	12	5
	>28	0	6	19
Tumor diameter***:	≤2 cm	6	2	1
	>2 cm	5	16	23
Capsule formation:	Present	11	16	20
	Absent	0	2	4
Capsule invasion:	Present	11	15	20
	Absent	0	3	4
Portal vein invasion:	Present	5	7	14
	Absent	6	11	10
Non-cancerous tissue:	Liver cirrhosis	6	10	7
	Chronic hepatitis	5	8	17
Intrahepatic metastasis:	Present	1	6	8
	Absent	10	12	16

–: negative. +: low-expression. ++: high-expression. *$P < 0.05$. **$P < 0.001$. ***$P < 0.01$.

Mina53 expression was observed in the nuclei of bile duct epithelium and of some of the lymphocytes infiltrating into portal areas. *Mina53* expression was also observed in compressed hepatocytes just around tumor nodules, and in those around portal areas when active interface hepatitis was present (Fig. 1c,d).

Diffuse or sometimes scattered expression of *mimitin* was often observed in the cytoplasm of HCC cells in tumor nodules (Fig. 1e). Non-cancerous tissues expressed *mimitin* in bile duct epithelium, and in scattered round cells in portal areas or fibrous areas (Fig. 1f). Some of the latter cells had Giemsa stain-positive granules in the cytoplasm, suggesting they are mast cells.

The positive cell area and intensity of *Mina53* or *mimitin* expression were larger and higher, respectively, in HCC cells than in non-HCC tissues.

Strong MIB-1 expression was often observed in the nuclei of HCC cells at the periphery of tumor nodules (Fig. 1g), and some cases had the expression in portal vein tumor thrombi (data not shown). In non-cancerous tissues, MIB-1 was expressed in the hepatocytes around tumor nodules and periphery of regenerative nodules (Fig. 1h), bile duct epithelium, and lymphocytes around portal areas.

Mina53 and MIB-1 expressions were localized in the nuclei, but in both cancerous and non-cancerous tissues of most cases, *Mina53* expression was higher than MIB-1.

Mina53 expression and clinicopathological factors (Table 1)

Mina53 expression level was negative (–) in 11 cases (20.7%, 3 well+moderately differentiated cases and 8 moderately differentiated cases), low-expression (+) in 18 cases (34.0%, 3 well+moderately differentiated, 12 moderately differentiated, 2 moderately+poorly differentiated, and one poorly differentiated), and high-expression (++) in 24 cases (45.3%, 15 moderately differentiated, 7 moderately+poorly differentiated, and 2 poorly differentiated). *Mina53* expression was weak in well-differentiated HCCs and strong in poorly differentiated HCCs. Statistically significant difference among the 3 expression levels was observed ($P < 0.05$).

MIB-1 index was low in the cases with weak *Mina53* expressions, high in cases with strong *Mina53* expressions, and the statistical significance ($P < 0.001$) was obtained.

Tumor diameter was ≤2 cm in many cases with weak *Mina53* expressions, while it was >2 cm in many cases with strong expression. Number of cases with >2 cm of diameter increased along with the increase in *Mina53* expression level, and the statistical significance

Table 2 Relationship between clinicopathological factors and *mimitin* expression in hepatocellular carcinoma ($n = 53$)

Mimitin expression level		–	+	++
Histological grade:				
Well+moderately differentiated		1	4	1
Moderately differentiated		7	11	17
Moderately+poorly differentiated		1	3	5
Poorly differentiated		1	1	1
MIB-1 index (%):	≤28	7	10	14
	>28	3	9	10
Tumor diameter:	≤2 cm	3	2	3
	>2 cm	7	17	21
Capsule formation:	Present	10	15	22
	Absent	0	4	2
Capsule invasion:	Present	10	14	22
	Absent	0	5	2
Portal vein invasion:	Present	4	10	12
	Absent	6	9	12
Non-cancerous tissue:	Liver cirrhosis	3	8	12
	Chronic hepatitis	7	11	12
Intrahepatic metastasis:	Present	0	8	7
	Absent	10	11	17

–: negative. +: low-expression. ++: high-expression.

($P < 0.01$) was obtained between the 3 expression level groups.

Frequency of portal vain invasion was tended to be high in the cases with strong *Mina53* expression, but there was no significant difference. Statistical significance was not observed either between *Mina53* expression and capsule formation, capsule invasion, or background diseases in non-cancerous tissues.

Mimitin expression and clinicopathological factors (Table 2)

Mimitin expression was negative (–) in 10 cases (18.9%, one well+moderately differentiated case, 7 moderately differentiated cases, one moderately+poorly differentiated case and one poorly differentiated case), low-expression (+) in 19 cases (35.8%, 4 well+moderately differentiated, 11 moderately differentiate, 3 moderately+poorly differentiated and one poorly differentiated), and high-expression (++) in 24 cases (45.3%, one well+moderately differentiated, 17 moderately differentiated, 5 moderately+poorly differentiated, and one poorly differentiated).

No significant differences were obtained between *mimitin* expression and histological grade or MIB-1 index.

Average tumor diameter increased from 32.9 mm in the negative expression group to 42.6 mm in the low-expression group, and 43.7 mm in the high-expression group, but there was no significant difference. There were no significant relationships to the other clinicopathological factors such as capsule formation and capsule invasion.

DISCUSSION

IMMUNOHISTOCHEMICAL STAININGS FOR *Mina53*, *mimitin* and MIB-1 were conducted on 53 HCC cases, and the relationship between their expressions and clinicopathological factors were examined.

Mina53 expression was reported to have a relationship with MIB-1 (an immunohistochemical proliferation marker) index in esophageal and colonic cancer tissues,[12,13] and suppression of *Mina53* expression *in vitro* by *Mina53*-specific small interfering RNA (siRNA) suppressed proliferation of esophageal and colorectal cancer cell lines. In the human colon cancer cell line SW620, suppression of *c-myc* expression by *c-myc*-specific siRNA suppressed *Mina53* expression, and this suggested direct involvement of *c-myc* in *Mina53* expression.[13]

To date, *Mina53* expression in HCC was not reported in the tissues level, but the relationships between *c-myc* and HCC were studied, e.g. *c-myc* expression is higher in HCC than normal liver,[17] higher in HCC with a large diameter or high proliferative capability,[18] and higher in HCC with multiple nodules than with single nodule.[19]

In our present immunohistochemical study, the positive cell area and intensity of *Mina53* expression were smaller and lower, respectively, in non-neopastic cells than HCC cells.

In HCC tissues, *Mina53* expression was observed diffusely in cancer cells in tumor nodules, and it was often observed strongly in HCC cells at the periphery of tumor nodules, and the expression level was related to MIB-1 index. In addition, the expression level was high in HCC at a low histological level and in HCC that diameter was >2 cm. We examined *Mina53* expression in 5 cases of HCC showing "nodule-in-nodule" appearance and found the strongest expression in less-differentiated HCC tissues in the central area (data not shown). These findings suggest that *Mina53* expression is related to biological malignancy and cell proliferation in HCC. In colon cancer tissues, *Mina53* expression was higher than MIB-1 expression,[13] and a similar tendency was observed in our HCC cases with *Mina53* expressions.

In non-HCC tissues, *Mina53* and MIB-1 were expressed in hepatocytes at the periphery of regenerative nodules and in compressed hepatocytes, but *Mina53* expression was higher than MIB-1. Bile duct epithelium and some of the lymphocytes express *Mina53*, but do not expresse MIB-1. In the non-cancerous region of renal cell carcinoma, *Mina53* was diffusely positive in normal tubules, but MIB-1 was generally negative.[20] In the non-cancerous tissues of esophageal carcinoma, *Mina53* expressions were found in the layers from the basal to the suprabasal, while MIB-1 expressions were found in the basal or epibasal areas.[12] In non-cancerous tissues of colon cancer, MIB-1 was expressed in the normal cells of crypt and lymphoid germinal center, while *Mina53* expressions were only sometimes observed.[13] These data suggest that in non-cancerous areas, *Mina53* expressions does not always coincide with MIB-1 expressions, and may not be regarded as having the same function as that of involvement in cancer cell proliferation as we previously speculated.[20]

MIB-1 is expressed during G1, S, G2 and M phases of cell cycle.[21–23] *Mina53* is a *myc*-target gene, and *c-myc* is expressed continuously in all phases of cell cycle in proliferating cells.[13] However, *Mina53* expression induced by *c-myc* is thought to occur in the proliferation of specific cells.

Relationship between *Mina53* expression and survival rate was studied in esophageal squamous cell carcinoma (ESCC),[12] renal cell carcinoma,[20] and neuroblastoma.[24] These studies reported higher survival rates in the cases with low *Mina53* expressions. However, our findings in this current study did not show significant relationship between *Mina53* expression and survival rate. On the other hand, relationship between *c-myc* expression and recurrence was observed in HCC,[18] but not in our findings.

In ESCC and other cancerous tissues, *Mina53* expression was involved to cell proliferation and related to survival rate and MIB-1 index, but *Mina53* expression and MIB-1 expression in non-cancerous area of cancerous tissues varied between studies. This suggested that *Mina53* is not a single regulative factor in cell proliferation, but various factors together with *Mina53* are involved in proliferation.

MIB-1 index increased with the progress of disease conditions, i.e. from normal liver tissues, hepatitis, liver chirrhosis, and then to HCC.[25] MIB-1 index is also reported to have a relationship to clinicopathological factors of HCC such as histological grade, survival rate, intrahepatic metastasis;[26] and to the HCC marker PIVKA-II, β-catenin that takes a role in cell-cell adhesion,[27] and ubiquitin that involves to protein repair and proteolysis.[28] In our current study, significant relationship was observed between MIB-1 index and such clinicopathological factors as histological grade, tumor diameter and intrahepatic metastasis, but not with survival rate and recurrence rate. King *et al.*[29] and Schmitt-Graff *et al.*[25] also examined survival and recurrence rates for ≥10% or <10% of MIB-1 levels, and they only indicated a possible relationship between patient prognosis and MIB-1 index. Grouping of MIB-1 index levels would need further investigation.

Suppression of *mimitin* expression in the ESCC cell line TE-11 by using *mimitin*-specific siRNA suppressed cell proliferation.[11] In ESCC tissues, *mimitin* was highly expressed, and the expression level was significantly correlated with the increase of MIB-1 index, but not with histological grade or age of patients.[11]

In HCC tissues of our current study, *mimitin* was expressed in varying degrees, but the expression was not correlated with cell proliferation as shown in ESCC, and it was not correlated with such clinicopathological factors as histological grade and tumor diameter.

In our current study, *Mina53* expression was more closely related to clinicopathological factors than *mimitin* expression. Tsuneoka *et al.* reported that the suppression of *mimitin* by using *mimitin*-specific siRNA in the HCC cell line KYN-2 did not inhibit cell proliferation.[11] These findings suggest that *Mina53* is more closely related to cell proliferation in HCC than *mimitin*.

Better understanding of *myc*-family gene expressions would help better management of neoplastic diseases. Identification and characterization of *myc*-specific target

genes such as *Mina53* and *mimitin* would help control cell proliferation, and open up a new frontier in cancer treatment.

REFERENCES

1 Tabor E. Tumor suppressor genes, growth factor genes, and oncogenes in hepatitis B virus-associated hepatocellular carcinoma. *J Med Virol* 1994; **42**: 357–65.
2 Caselmann WH. Transactivation of cellular gene expression by hepatitis B viral proteins: a possible molecular mechanism of hepatocarcinogenesis. *J Hepatol* 1995; **22**: 34–7.
3 Rogler CE, Chisari FV. Cellular and molecular mechanisms of hepatocarcinogenesis. *Semin Liver Dis* 1992; **12**: 265–78.
4 Marcu KB, Bossone SA, Patel AJ. Myc function and regulation. *Annu Rev Biochem* 1992; **61**: 809–60.
5 Morgenbesser SD, DePinho RA. Use of transgenic mice to study myc family gene function in normal mammalian development and in cancer. *Semin Cancer Biol* 1994; **5**: 21–36.
6 Henriksson M, Luscher B. Proteins of the Myc network: essential regulators of cell growth and differentiation. *Adv Cancer Res* 1996; **68**: 109–82.
7 Grandori C, Cowley SM, James LP, Eisenman RN. The Myc/Max/Mad network and the transcriptional control of cell behavior. *Annu Rev Cell Dev Biol* 2000; **16**: 653–99.
8 Lutz W, Leon J, Eilers M. Contributions of Myc to tumorigenesis. *Biochim Biophys Acta* 2002; **1602**: 61–71.
9 Tsuneoka M, Ras MekadaE. /MEK signaling suppresses Myc-dependent apoptosis in cells transformed by c-myc and activated ras. *Oncogene* 2000; **19**: 115–23.
10 Tsuneoka M, Koda Y, Soejima M, Teye K, Kimura H. A novel myc target gene, *Mina53*, that is involved in cell proliferation. *J Biol Chem* 2002; **277**: 35450–9.
11 Tsuneoka M, Teye K, Arima N *et al.* A novel Myc-target gene, *mimitin*, that is involved in cell proliferation of esophageal squamous cell carcinoma. *J Biol Chem* 2005; **280**: 19977–85.
12 Tsuneoka M, Fujita H, Arima N *et al. Mina53* as a potential prognostic factor for esophageal squamous cell carcinoma. *Clin Cancer Res* 2004; **10**: 7347–56.
13 Teye K, Tsuneoka M, Arima N *et al.* Increased expression of a Myc target gene *Mina53* in human colon cancer. *Am J Pathol* 2004; **164**: 205–16.
14 Yaswen P, Goyette M, Shank PR, Fausto N. Expression of c-Ki-ras, c-Ha-ras, and c-myc in specific cell types during hepatocarcinogenesis. *Mol Cell Biol* 1985; **5**: 780–6.
15 Thompson NL, Mead JE, Braun L, Goyette M, Shank PR, Fausto N. Sequential protooncogene expression during rat liver regeneration. *Cancer Res* 1986; **46**: 3111–17.
16 Zhang XK, Huang DP, Qiu DK, Chiu JF. The expression of c-myc and c-N-ras in human cirrhotic livers, hepatocellular carcinomas and liver tissue surrounding the tumors. *Oncogene* 1990; **5**: 909–14.
17 Arbuthnot P, Kew M, Fitschen W. c-fos and c-myc oncoprotein expression in human hepatocellular carcinomas. *Anticancer Res* 1991; **11**: 921–4.
18 Kawate S, Fukusato T, Ohwada S, Watanuki A, Morishita Y. Amplification of c-myc in hepatocellular carcinoma: correlation with clinicopathologic features, proliferative activity and p53 overexpression. *Oncology* 1999; **57**: 157–63.
19 Wang Y, Wu MC, Sham JS, Zhang W, Wu WQ, Guan XY. Prognostic significance of c-myc and AIB1 amplification in hepatocellular carcinoma. A broad survey using high-throughput tissue microarray. *Cancer* 2002; **95**: 2346–52.
20 Ishizaki H, Yano H, Tsuneoka M *et al.* Overexpression of the myc target gene *Mina53* in advanced renal cell carcinoma. *Pathol Int* 2007; **57**: 672–80.
21 Gerdes J, Lemke H, Baisch H, Wacker HH, Schwab U, Stein H. Cell cycle analysis of a cell proliferation-associated human nuclear antigen defined by the monoclonal antibody Ki-67. *J Immunol* 1984; **133**: 1710–15.
22 Lopez F, Belloc F, Lacombe F *et al.* Modalities of synthesis of Ki67 antigen during the stimulation of lymphocytes. *Cytometry* 1991; **12**: 42–9.
23 Bruno S, Darzynkiewicz Z. Cell cycle dependent expression and stability of the nuclear protein detected by Ki-67 antibody in HL-60 cells. *Cell Prolif* 1992; **25**: 31–40.
24 Fukahori S, Yano H, Tsuneoka M *et al.* Immunohistochemical expressions of Cap43 and *Mina53* proteins in neuroblastoma. *J Pediatr Surg* 2007; **42**: 1831–40.
25 Schmitt-Graff A, Ertelt V, Allgaier HP *et al.* Cellular retinol-binding protein-1 in hepatocellular carcinoma correlates with beta-catenin, Ki-67 index, and patient survival. *Hepatology* 2003; **38**: 470–80.
26 Morinaga S, Ishiwa N, Noguchi Y *et al.* Growth index, assessed with Ki-67 and ssDNA labeling; a significant prognosticator for patients undergoing curative resection for hepatocellular carcinoma. *J Surg Oncol* 2005; **92**: 331–6.
27 Inagawa S, Itabashi M, Adachi S *et al.* Expression and prognostic roles of beta-catenin in hepatocellular carcinoma: correlation with tumor progression and postoperative survival. *Clin Cancer Res* 2002; **8**: 450–6.
28 Shirahashi H, Sakaida I, Terai S, Hironaka K, Kusano N, Okita K. Ubiquitin is a possible new predictive marker for the recurrence of human hepatocellular carcinoma. *Liver* 2002; **22**: 413–18.
29 King KL, Hwang JJ, Chau GY *et al.* Ki-67 expression as a prognostic marker in patients with hepatocellular carcinoma. *J Gastroenterol Hepatol* 1998; **13**: 273–9.

RecQL1 DNA repair helicase: A potential tumor marker and therapeutic target against hepatocellular carcinoma

KAZUNOBU FUTAMI[1], SACHIKO OGASAWARA[2], HIDEYUKI GOTO[1], HIROHISA YANO[2] and YASUHIRO FURUICHI[1]

[1]GeneCare Research Institute Co., Ltd., 19-2 Kajiwara, Kamakura, Kanagawa 247-0063; [2]First Department of Pathology, Kurume University School of Medicine, 67 Asahi-machi, Kurume, Fukuoka 830-0011, Japan

Received November 30, 2009; Accepted December 29, 2009

DOI: 10.3892/ijmm_00000375

Abstract. RecQL1 in the human RecQ DNA helicase family participates in DNA repair and recombination pathways in cell cycle replication. Immunohistochemical analysis of human hepatocellular carcinoma (HCC) tissues showed that RecQL1 expression is strongly correlated with histological grade and MIB-1 indices of HCC, and that the expression was greater in simple HCCs inducing extranodular growth or portal vein invasion than in HCCs not inducing extranodular growth or portal vein invasion. These histological data reveal the potential of RecQL1 as a biological marker predicting the malignancy and progression of liver cancer. High expression profiles were also produced by various HCC cells, including HCC cell lines established by us. When RecQL1 expression was silenced by siRNA *in vitro*, most HCC cells died of mitotic catastrophe. In a mouse orthotopic xenograft model of liver cancer with transplanted human HCC, RecQL1-siRNA mixed with cationic liposomes exhibited a strong anticancer effect that prevented the growth of the cancer. RecQL1-siRNA inhibited the growth of human HCC in the mouse liver, confirming that RecQL1 is an excellent molecular agent against liver cancer and suggests that RecQL1-siRNA formulated with liver-prone liposomes has excellent potential as a therapeutic drug against liver cancers.

Introduction

Human hepatocelullar carcinoma (HCC) is one of the most common tumors worldwide. The prognosis of HCC patients remains poor, and thus identifying useful therapeutic targets and prognostic markers are urgently required, although a dominant pathway has not been found responsible for the development of HCC (1). Liver-specific neoplasms arise under various physiological backgrounds and from virus infection that results in many types of cellular chromosome aberrations, gene mutations, epigenetic alterations and altered signaling pathways. Studies have shown that alterations of cell cycle regulators occur in HCC (2), particularly in structural or functional modifications in genes such as TP53, Rb1, P16/INK4a and P21/WAF1, participating in the DNA damage response system (3-10).

The RecQL1 (also known as RecQL or RecQ1) helicase, a member of the RecQ DNA helicase family participating in genomic stability, is expressed highly in proliferating cells. Functionally, down-regulation of RecQL1 in HeLa cells by RNA interference increases sister chromatid exchanges (11). RecQL1-deficient mice produced by gene targeting are indistinguishable from wild-type mice except that embryonic fibroblasts from RecQL1-deficient mice are sensitive to ionizing radiation (12). These findings collectively indicate that the RecQL1 helicase suppresses chromosomal instability by participating in DNA repair during the cell cycle, but its function seems to be nonessential, since no human disease is known to be related to its gene mutation. Previously, we found that cancer cells were extremely sensitive to RecQL1 silencing by RNA interference with small interfering RNA (siRNA) and that cell growth was severely inhibited, as if these cancer cells were addicted to highly expressed RecQL1. Yet, non-cancerous cells and all normal cells tested were unaffected by RecQL1-specific RNA interference (13,14). This unique event was idenitfied as mitotic catastrophe during mitosis of the cell cycle in checkpoint system-deficient cancer cells due to accumulation of DNA damage caused by the absence of the RecQL1 helicase (14). To use this cancer cell-specific killing mechanism for the clinical benefit of anticancer chemotherapy, preliminary trials using model mice inoculated with various human cancer cells have been carried out (15).

In the present study, we focused our study on RecQL1 in hepatic cancers. First, we investigated the expression level of RecQL1 protein in clinically obtained HCCs (~40 cases) to ascertain whether the expression level of the RecQL1 helicase is directly related to differentiation of HCC cells, malignancy of cancer cells and patient prognosis. Second, by using several HCC cell lines which included three HCC cell lines

Correspondence to: Dr Yasuhiro Furuichi, GeneCare Research Institute Co., Ltd., 19-2 Kajiwara, Kamakura, Kanagawa 247-0063 Japan
E-mail: furuichi@genecare.co.jp

Abbreviations: HCC, hepatocellular carcinoma; siRNA, small interfering RNA

Key words: hepatocelullar carcinoma, DNA damage, RNA interference, mitotic catastrophe, anti-cancer siRNA drug

established in our laboratory (16-20), we studied the effect of RecQL1 silencing on cell proliferation *in vitro*. Third, we set up a mouse orthotopic hepatoma model with human HCC cells, and the anticancer efficacy of the RecQL1-siRNA/cationic liposome complex was examined *in vivo* to assess whether RNA interference therapy is able to be used in the management of hepatic cancers. The results are discussed considering the possible use of RecQL1 expression as a developmental marker of hepatic cancer and of RecQL1-siRNA as an anti-hepatic cancer drug.

Materials and methods

Pathological analysis of the expression of the RecQL1 helicase in human HCCs. Immunohistochemical examination of the RecQL1 helicase was performed by using paraffin sections of HCC and non-HCC tissues obtained with written consent from 40 HCC patients who were surgically resected between 1994 and 1996 at Kurume University Hospital, Japan. The anti-RecQL1 antibody Q1N3, which was generated by us and was confirmed to be specific for the N-terminal domain of RecQL1 helicase (amino acid residues 1-338) and the Signal-Amplification System II (code K1497, Dako, Ely, UK) were used. The patients had no chemotherapeutic treatment before surgery. Four tissues were from hepatic B virus carriers, 27 tissues were from hepatic C virus carriers and 1 tissue was from a patient infected with both hepatic B and C viruses. HCC tissue samples consisted of 4 well to moderately differentiated HCCs, 28 moderately differentiated HCCs, 7 moderately to poorly differentiated HCCs, and 1 poorly differentiated HCC. The proliferation activity of HCC cells was monitored using Ki-67 expression as an MIB-1 index. For the evaluation standard of RecQL1, we used RecQL1-positive bile duct epithelium in the same specimen (positive internal control). The specimen was evaluated as low expression (+) when it was stained as intensively as the positive internal control, as high expression (++) when the staining was more intensive, and as negative (-) when it was not stained at all. We examined the relationship between RecQL1 expression and the clinicopathological features of the HCC cases, such as histological grade, MIB-1 index, tumor size, portal vein invasion and intrahepatic metastasis. Pathological features were evaluated according to the classification of the Liver Cancer Study Group of Japan. Statistical analyses were carried out for each clinicopathological characteristic among the (-), (+) and (++) groups.

The relationships between RecQL1 expression and histological grades, and between RecQL1 expression and the MIB-1 index were examined by using the Jonckheere-Terpstra test. The relationships between RecQL1 expression and recurrence or survival rate were evaluated by using the Fisher's exact P-test or by using the log-rank test, respectively. The relationships between RecQL1 expression and other clinicopathological features were examined by using the Kruskal-Wallis test.

Cells and cell culture conditions. HCC cell lines (HepG2, Hep3B, Huh7, SK-HEP-1, Li-7, HAK-1A, HAK-1B, KIM-1, KYN-1, KYN-2 and KYN-3) and normal cell lines ARPE19 (a normal spontaneously arising retinal pigmented epithelium cell line) and TIG-3 (normal lung diploid fibroblasts from human fetuses) were used. HepG2, Hep3B, SK-HEP-1, ARPE19 were obtained from ATCC (Manassas, VA, USA). Huh7 and Li-7 were obtained from Riken Cell Bank (Tsukuba, Japan). TIG-3 was obtained from the Japan Health Sciences Foundation (Osaka, Japan). The remaining six HCC cell lines were originally established by us from surgically resected HCC nodules at Kurume University, Japan. KIM-1 (16) and KYN-1 (17) were established from moderately differentiated HCC nodules, KYN-2 was established from moderately to poorly differentiated HCC nodules (18) and KYN-3 was established from peritoneal effusion of HCC patients with moderately to poorly differentiated HCC (19). HAK-1A and HAK-1B were established from a single HCC nodule showing a three-layered structure with a different histological grade in each layer (20). These cell lines were previously confirmed to retain the morphological and functional characteristics of the original tumor.

The cells were grown in Dulbeco's modified Eagle's or RPMI-1640 medium (Nacalai Tesque, Kyoto, Japan) and were incubated at 37°C in a humidified chamber supplemented with 5% CO_2. Some cells were treated with genotoxic agent doxorubicin (Adriamycin; Sigma, St. Louis, MO, USA) at the concentration 0.25 μM for 24 h at 37°C.

siRNA and RNA interference. siRNAs (21 bp) targeting RecQL1 mRNA (RecQL1-siRNA) and negative control siRNA (NS-siRNA) were chemically synthesized (Nippon EGT, Toyama, Japan). All siRNA sequences had an overhanging 3'-dTdT at the 3' terminus (14). Sequence-specific gene silencing was confirmed by using cDNA microarray analysis with the Affymetrix GeneChip system (Human Genome U133 Plus 2.0 Array). For transfection at 24 h after plating, the cells were incubated with 40 nM siRNA duplex for 8 h in the presence of RNAiMax (Invitrogen, Carlsbad, CA, USA) and were cultured in fresh medium.

Reverse transcriptase-PCR. After transfection, total RNA was extracted from cultured cells by using an RNeasy Mini Kit (Qiagen GmbH, Hilden, Germany) according to the manufacturer's protocol. Reverse transcriptase-PCR analyses were carried out by using the ABI PRISM 7000 Sequence Detection System with TaqMan probes and primers (ABI, Foster, CA, USA). The ß-actin gene was used as the internal standard (TaqMan probe ID; 431088E; ABI). RecQL1 silencing was monitored by using a specific primer set (Hs00262956_m1). Expression of genes P16/INK4a (CDKN2A), Hs00233365_m1; P21/WAF1 (CDKN1A), Hs00355782_m1; P27/KIP1 (CDKN1B), Hs00153277_m1; TP53; Hs00153340_m1; and Rb1, Hs01078066_m (ABI) were also determined and were used as references.

Cell proliferation assays. Cell proliferation was measured by using colorimetric assays based on the cleavage of tetrazolium salt WST-8 (Nacalai Tesque). The absorbance of the formazan dye formed was measured at 450 nm at 3 h after adding the reagent.

Flow cytometric analysis. Trypsin-treated cells were washed with phosphate-buffered saline (PBS) and were fixed in ice-

cold methanol for 2 h. The cells were treated with pancreatic RNase A (Nippon Gene, Toyama, Japan) and stained with propidium iodide (Sigma) for 30 min. The cells were then analyzed by using flow cytometry. Fluorescence was measured by using Epics XL (Beckman Coulter K.K., Tokyo, Japan). For each sample, 10,000 events were analyzed.

Immunoblotting. The protein levels of RecQL1 and other proteins participating in the cellular DNA damage repair system were monitored by using immunoblot analysis. The cells were washed with ice-cold PBS, were pelleted and then were lysed in a sodium dodecyl sulfate (SDS) buffer containing 1% SDS, 2% ß-mercaptoethanol, 20% glycerol, 30 mM Tris-HCl (pH 6.8) and 0.2 M dithiothreitol. The cell lysate was boiled for 10 min and then was electrophoresed on 5-20% gradient SDS-polyacrylamide gels. Proteins fractionated on the gels were electrophoretically transferred to poly-vinylidene difluoride membranes (Immobilon, Millipore, MA, USA) and were blocked overnight with 5% skimmed milk in PBS. The membranes were then incubated with either anti-RecQL1 monoclonal antibody Q1N3 or anti-ß-actin monoclonal antibody (ICN Biomedicals, Aurora, OH, USA) for 60 min at room temperature. Antibodies detecting TP53 (DO-1), P21/WAF1 (Ab-1), PCNA and Rb1 proteins were purchased from Santa Cruz Biotechnology (Santa Cruz, CA, USA), Oncogene (San Diego, CA, USA), Abcam Limited (Cambridge, UK) and Cell Signaling Technology (Danvers, MA, USA), respectively, and were used to detect the proteins important in oncology. The membranes were washed with 0.05% Tween-20 in PBS, incubated with anti-mouse IgG conjugated with horseradish peroxidase (DakoCytomation, Carpinteria, CA, USA) and washed. They were subsequently developed using an enhanced chemiluminescence reagent (ECL Plus, Amersham Biosciences, UK).

Orthotopic implantation in mice. Mice (BALB/c $nu^{+/+}$) purchased from Charles River Japan, Inc. (Yokohama, Japan) were maintained in a pathogen-free environment. They received humane care in accordance with the National Institutes of Health Guide for the Care and Use of Laboratory Animals.

The orthotopic hepatoma model of mice was designed according to the method of Lu *et al* (21). Briefly, KYN-2 cells ($2.0x10^6$) were harvested from subconfluent cultures and were suspended in serum-free medium containing 50% Matrigel (BD Bioscience, Bedford, MA, USA). The cells were slowly injected into the mouse liver through the diaphragmatic surface by using a 28-gauge needle. The skin was then closed with an absorbable suture and sterile surgical clips. On day 7 after the cell injections, mice with established intrahepatic tumors were randomized into three groups (each group n=10-11) and received therapeutic treatments of the siRNA/cationic liposome complex from day 7.

Intravenous injection of the RecQL1-siRNA/LIC-101 complex. The RecQL1-siRNA/LIC-101 complex was prepared by Nippon Shinyaku Co., Ltd. (Kyoto, Japan) as previously described (22). The RecQL1-siRNA/LIC-101 complex (2 mg siRNA/kg mouse body weight, equivalent to ~50 μg siRNA/mouse) in 100 μl of 10% (w/v) maltose solution, was injected intravenously once on days 7, 9, 11, 14, 16, 18, 21, 23, 25, 28, 30 and 32, a total of 12 injections. The anticancer effects were evaluated on day 35. The average liver weights were analyzed by using the Dunnett's test.

Results

RecQL1 expression in various HCCs and the relationship to clinicopathological MIB-1 features of HCC. RecQL1 was expressed to various degrees in most HCC nodules (82.5% of the 40 HCC specimens) (Fig. 1A and B). RecQL1 expression was high around the peripheral area of the HCC nodules in some cases. Tumor thrombi in the portal vein showed relatively strong RecQL1 expression. In non-cancerous areas, the RecQL1 expression was also observed in infiltrating lymphocytes, endothelial cells and hepatocytes to various degrees (Fig. 1C and D). The degree of RecQL1 expression was evaluated as negative (-) in 7 (3 well to moderately differentiated, 4 moderately differentiated; 17.5%), low expression (+) in 15 (1 well to moderately differentiated, 13 moderately differentiated, 1 moderately to poorly differentiated; 37.5%), and high expression (++) in 18 (11 moderately differentiated, 6 moderately to poorly differentiated, 1 poorly differentiated; 45.0%) HCC cases (Table I). Upon analysis of the relationship between RecQL1 expression and clinicopathological features (Table I, Fig. 2), we found that RecQL1 expression was: i) significantly correlated with histological grade and MIB-1 indices of the HCCs; ii) significantly higher in the simple nodular type HCC cases (with extranodular growth) than in the HCCs without extranodular growth; iii) significantly higher in the HCC cases with portal vein invasion than in the HCCs without portal vein invasion; and iv) higher in the HCC nodules of diameter ≥2.0 cm than in the HCC nodules of diameter <2.0 cm. RecQL1 expression and other clinicopathological features, such as prognosis, including recurrence and survival time of patients, showed no apparent relationship.

RecQL1 helicase expression levels in various HCC cell lines. RecQL1 expression in various HCC cell lines was investigated. As controls, normal cells ARPE19 and TIG-3 were similarly characterized. Most HCC cells expressed a greater amount of RecQL1 helicase protein than the normal cells (Fig. 3A). RecQL1 expression was exceptionally high in the Li-7, SK-HEP-1, HAK-1A, HAK-1B, KYN-2 and KYN-3 HCC cell lines.

To understand the expression of other genes participating in DNA repair and the cell cycle, HCC cells were treated with genotoxic agent doxorubicin and the induced proteins were characterized (Fig. 3A). TP53, which is a DNA damage sensor, was not expressed in Hep3B, Li-7, KIM-1 and KYN-2 cells in the absence of doxorubicin, nor after doxorubicin treatment [TP53 vs. TP53 (Dox)] (Fig. 3A). In the KYN-1 cells, TP53 expression remained high, even in the absence of doxorubicin, suggesting that the TP53 gene mutates to an inactive form and so may not be able to contribute to genomic stability. The TP53 gene mutates in HCC cells KYN-1, KYN-3, HAK-1A and HAK-1B (20) and it mutates in SK-HEP-1 and Huh7 cells, but induction of the TP53 expression after DNA damage seems to be unaffected (23). In the present study,

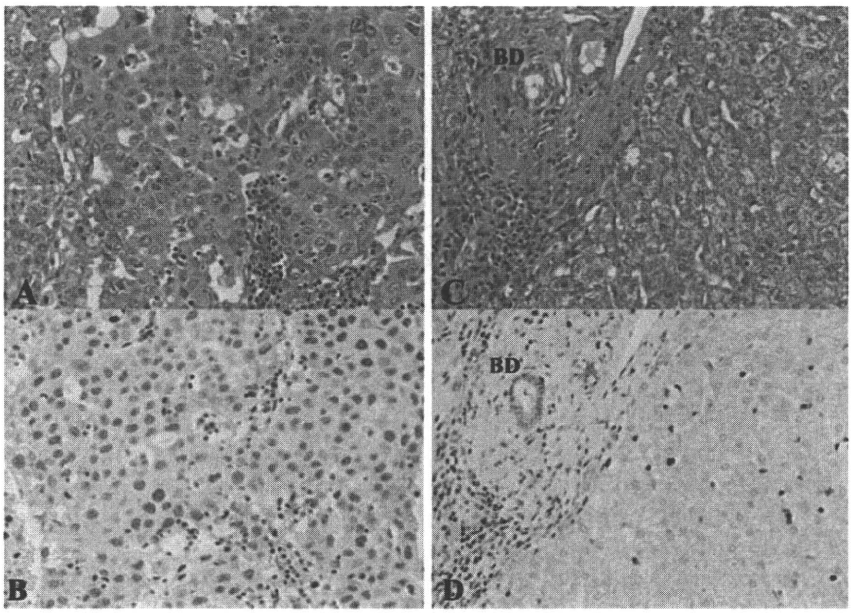

Figure 1. Immunohistochemical staining of RecQL1 in HCC and non-HCC tissues. (A) Moderately to poorly differentiated HCC stained with hematoxylin and eosin (H&E) (x100). (B) RecQL-1 expression in the nuclei of HCC cells (x200). (C) non-HCC tissue with a bile duct (BD) in the portal tract (H&E) (x100). (D) RecQL-1 expression in bile duct epithelial cells and infiltrating lymphocytes in the portal tract, and endothelial cells in the sinusoid (x100).

TP53 gene expression appeared normal in HepG2 cells, as the TP53 expression was induced highly by doxo-rubicin treatment. In the normal cells, APRE19 and TIG-3, TP53 expression increased in response to DNA damage caused by the doxorubicin treatment.

Next, we investigated P21/WAF1 gene expression and its response to DNA damage by doxorubicin. The P21/WAF1 gene was expressed poorly in most HCC cells, except HepG2 and SK-HEP-1 cells, but it was highly expressed in ARPE19 and TIG-3 normal cells, indicating that P21/WAF1 may be a candidate HCC-specific tumor marker. P21/WAF1 is induced in cells containing wild-type TP53 when the cells are exposed to DNA damaging agents, but not in cells containing the mutant TP53. These data indicate that most of the HCC cell lines that we investigated contained an incomplete DNA repair system that otherwise should be activated by the TP53-P21/WAF1-mediated DNA damage signaling pathway. Also, Rb1 was not expressed in Hep3B cells. It should be emphasized that TP53, P21/WAF1 and Rb1 were expressed efficaciously in normal cells in response to DNA damage by doxorubicin (Fig. 3A), while they were not in most, if not all, HCC cell lines.

mRNA expression levels of TP53, Rb1, P16/INK4a and P21/WAF1 were compared among the various HCC cell lines by using reverse transcriptase-PCR analysis. TP53 was poorly expressed in Hep3B, Li-7, KIM-1 and KYN-2 cells, Rb1 was not expressed well in Hep3B cells, and the P16/INK4a gene was not expressed in Li-7 and SK-HEP-1 cells. Again, the P21/WAF1 mRNA expression was low in most, if not all, HCC cell lines and was consistent with the results from the Western blot analysis (Fig. 3A and B). The data clearly indicate that the G1/S checkpoint system was defective in these proliferating HCC cells, consistent with previous studies (2-10).

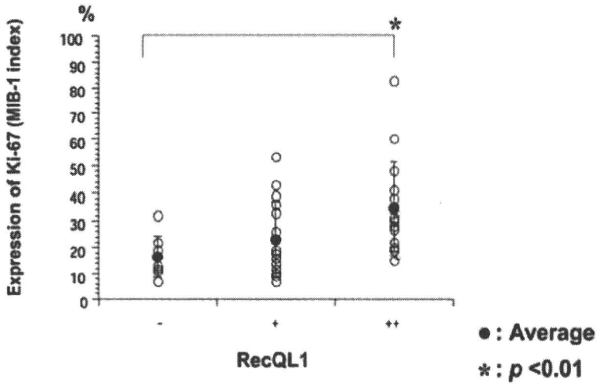

Figure 2. Relationship between RecQL1 and Ki-67 expression (MIB-1 index) in HCC. MIB-1 indices were compared in three different groups: RecQL1 negative group, RecQL1 low expression group, and RecQL1 high expression group. Their respective average MIB-1 indices were 16.6, 23.1 and 34.9%. Their averages are indicated by closed circles. A significant difference in MIB-1 indices was observed between the RecQL1 negative and RecQL1 high expression groups.

Induction of mitotic catastrophe in HCC cell lines by RecQL1 silencing. We investigated the effect of RecQL1 silencing in these HCC cell lines that lacked an intact DNA damage sensor and checkpoint system but replicated actively. To our surprise, RecQL1-siRNA killed a wide range of proliferating HCC cell lines efficaciously after it induced mitotic catastrophe. Fig. 4A shows the typical features of mitotic catastrophe observed in the KYN-3 cells. The KYN-3 cells clearly began to die as RecQL1 was silenced by siRNA treatment (Fig. 4C), resulting in accumulation of cells arrested at the M phase.

To define this cell-killing effect by RecQL1 silencing, time course experiments were performed with several HCC

Table I. RecQL1 expression and clinicopathological features in HCC.

RecQL1 expression	-	+	++
Histological grade[a]			
Well + Mod	3	1	0
Mod	4	13	11
Mod + Poor	0	1	6
Poor	0	0	1
MIB-1 index (%)[a]			
<14	4	5	0
14-27	2	5	6
28-51	1	4	10
>51	0	1	2
Tumor size			
≤2 cm	2	2	1
>2 cm	5	13	17
Macroscopic type			
Simple nodular type	7	12	8
Simple nodular type[b] with extranodular growth	0	3	10
Capsule formation			
(-)	1	1	1
(+)	6	14	17
Capsular invasion			
(-)	2	1	1
(+)	5	14	17
Portal vein invasion			
(-)	5	10	6
(+)[c]	2	5	12
Intrahepatic metastasis			
(-)	5	13	11
(+)	2	2	7
Non-cancerous tissue			
Chronic hepatitis	3	9	13
Liver cirrhosis	4	6	5

[a]RecQL1 expression was significantly ($P<0.001$) correlated with histological grade and MIB-1 indices of HCC cells. [b]$P<0.01$ vs. the simple nodular type. [c]$P<0.05$ vs. (-). Well, well-differentiated; Mod, moderately differentiated; Poor, poorly differentiated.

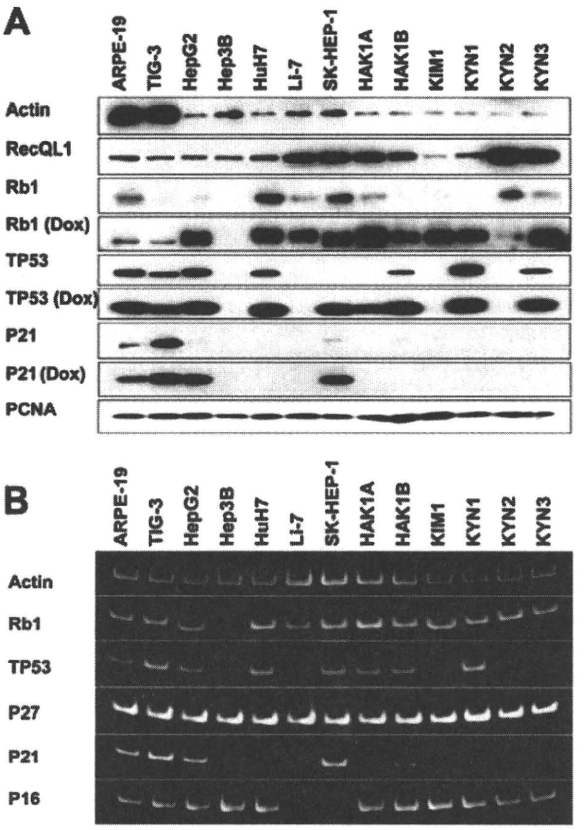

Figure 3. Expression of RecQL1 and cell cycle-related regulation genes in HCCs. (A) Cell lysates (10 μg) were applied to each lane. Proteins underwent Western blot analysis by using individual antibodies. The cellular induction of gene expression upon DNA damage was monitored by protein analysis before and after doxorubicin (Dox) treatment. (B) Quantitative analysis of gene expression by the determination of individual mRNAs with reverse transcriptase-PCR.

cell lines of various genetic backgrounds. The cells were incubated once with 40 nM siRNA and were cultured in siRNA-free medium for several days. HCC cell lines, such as SK-HEP-1, KYN-2 and KYN-3, began to die after a lag-time of about 48 h (Fig. 4B). In contrast, the growth of normal ARPE19 and TIG-3 cells that rapidly proliferated similar to HCC cell lines was almost unaffected despite RecQL1 gene silencing by RecQL1-siRNA (Fig. 4B). A slight retardation (10-15%) of growth was noted in these normal cell lines when compared with the non-silencing siRNA-treated cells.

Flow cytometric cell analysis showed a large peak correlated with the subG1 fraction representing debris associated with cell death in all RecQL1-siRNA-treated HCC cells. Some RecQL1-siRNA-treated HCC cells underwent unequal cell division after the arrested M phase, resulting in giant cells that could not divide and that looked like senesced cells (data not shown). This suggested that RecQL1-siRNA-treated HCC cells entered the M phase with no regulation and then developed mitotic catastrophe or aberrant cell division. In contrast, the normal cells, ARPE19 and TIG-3, showed no mitotic catastrophe because of premature arrest and repair at both the G1 and G2 phases. Non-silencing siRNA treatment under the same conditions did not affect the cell cycle progression of HCC and normal cells, indicating that cancer cell-specific mitotic catastrophe is dependent on RecQL1 silencing. Also, cancer cell-specific mitotic catastrophe is clearly dependent on replication of cells and genetic defects in HCC cells, such as the absence of P21/ WAF1 expression.

Effect of systemic administration of the RecQL1-siRNA/ LIC-101 complex in the KYN-2 orthotopic xenograft model in mice. We investigated the therapeutic efficacy of RecQL1-

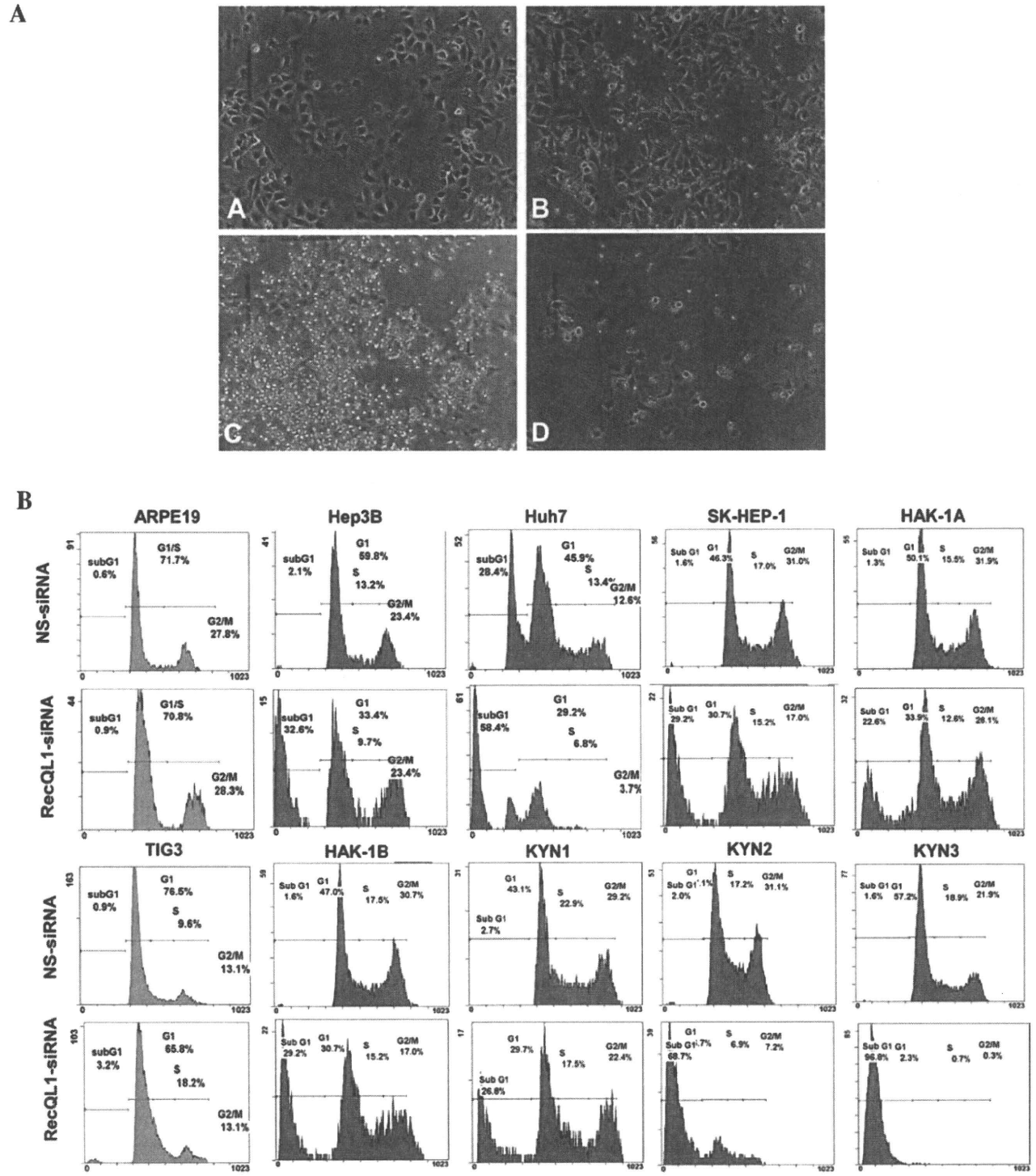

Figure 4A and B.

siRNA against KYN-2 cells in an orthotopic hepatoma model by using cationic liposome LIC-101 that carries siRNA to the cytosol of liver cells (22). In the *in vivo* experiments, the RecQL1-siRNA/LIC-101 complex was administered to mice which had formed KYN-2 nodules. Fig. 5A shows the KYN-2 tumors formed in the livers, and the results of therapeutic treatment with systemic injection of the RecQL1-siRNA/LIC-101 complex. KYN-2 tumors grew to a large volume in control mice that were injected with 10% maltose solution (Fig. 5B). KYN-2 tumors grew extensively in the liver of mice injected with the non-silencing siRNA/LIC-101 complex (Fig. 5C). However, only a few KYN-2 tumors appeared in the liver of mice treated with the RecQL1-siRNA/LIC-101 complex (Fig. 5D), indicating that RecQL1-siRNA effectively prevented the growth of KYN-2 tumors in the orthotopic hepatoma model. A clear statistical difference ($p<0.05$) in liver weight was observed between mice injected with 10% maltose or the non-silencing siRNA/LIC-101 complex and mice injected with the RecQL1-siRNA/LIC-101 complex (Fig. 5B).

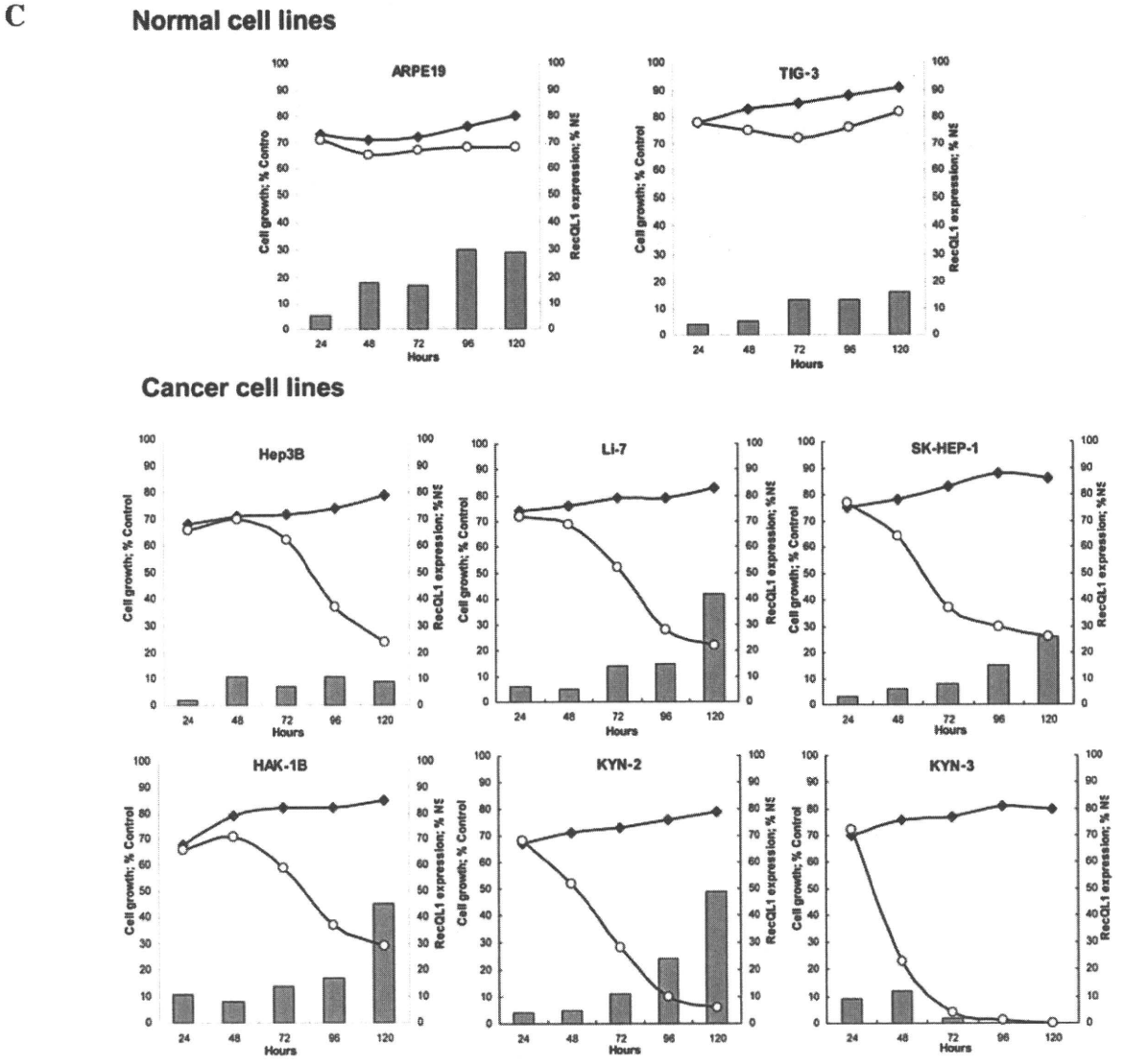

Figure 4. Growth inhibitory effect of RecQL1-siRNA on various HCC cells. (A) KYN-3 cells treated with RecQL1-siRNA. Microscopic features of cells were monitored at A, 24 h; B, 36 h; C, 48 h; and D, 72 h. (B) Flow cytometric analysis of HCC cells 72 h after siRNA treatment. (C) Time course analysis of viability of HCC cells and RecQL1 silencing. Six HCC cell lines (Hep3B, SK-HEP-1, LI-7, HAK-1B, KYN-2 and KYN-3) and two normal cell lines (TIG-3 and ARPE19) were transfected either with RecQL1-siRNA (open circle) or with NS-siRNA (solid circle). The viability of cells is shown as the relative growth to that of non-treated cells. The histograms show the relative expression level of RecQL1-silenced cells compared with the NS-siRNA-treated cells used as controls.

Discussion

Increased expression of RecQL1 in undifferentiated human HCC cells. The RecQL1 helicase has long been known to participate in DNA repair reactions, but little is known about its relation to human disease and the clinical outcome of therapy. Li *et al* (24) previously showed that single nucleotide polymorphisms of RecQL1 have a marked influence on the clinical response to therapy using genotoxic drugs and radiation, and to the overall survival of patients with pancreatic cancer. In this study, we investigated RecQL1 expression in clinical specimens of HCC and found that RecQL1 expression was significantly correlated with histological grade and MIB-1 indices of HCC development. RecQL1 expression and the MIB-1 index had a close relationship, suggesting that RecQL1 participates in cell proliferation, and, importantly, the RecQL1 expression profile resembled that of the well-known tumor marker PCNA of previous studies (25,26). These data verify that RecQL1 expression may be a reliable tumor marker, similar to PCNA, representing the progression and malignancy of cancers.

Incomplete regulation of the cell cycle in human HCC cells. HCC cells have a divergent and incomplete cell cycle regulation system that is perhaps compensated by a high expression of DNA repair enzymes to guarantee rapid and competent proliferation of cells (Fig. 3). In most of the HCC cell lines, expression of TP53 and P21/WAF1, which responds to DNA damage signaling and regulates cell cycle progression by inhibiting the cyclin-CDK complex, respectively, was severely reduced. This reduction also causes the inability of Rb1/E2F to reduce the transcription of genes promoting the cell cycle, resulting in the inability of G1/S arrest during cell cycle progression (27). Conceivably,

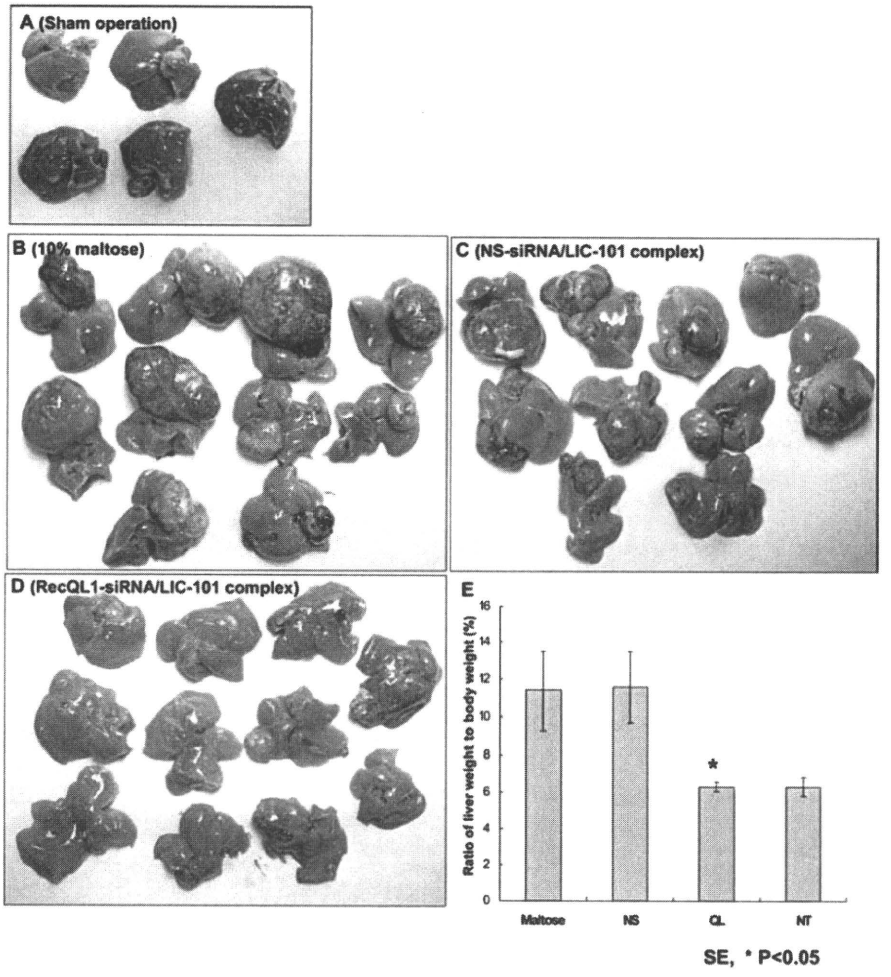

Figure 5. Therapeutic anticancer activity of RecQL1-siRNA in a mouse xenograft model of HCC. siRNA (2 mg/kg) formulated with LIC-101 cationic liposomes (suspended in 10% maltose) was injected intravenously into the tail vein of mice. (A) Sham operation mouse livers, (B) mouse livers treated with 10% maltose, (C) mouse livers treated with the NS-siRNA/LIC-101 complex, (D) mouse livers treated with the RecQL1-siRNA/LIC-101 complex, and (E) ratio of the weight of the liver to the weight of one mouse. Bars, the standard error of the measurements. *RecQL1-siRNA/LIC-101 complex is statistically more effective than the NS-siRNA/LIC-101 complex.

the absence of P21/WAF1 expression prevented the G1/S cell cycle stop due to lack of Rb1/E2F transcription initiation. These cell cycle defects found so far in many types of cancer cells exist in HCC, as shown in this study. Even in SK-HEP-1 cells in which the expression of P21/WAF1 appeared to be normal, P16/INK4a which is required to stop cell cycling, was not expressed (Fig. 3B). Here, the promoter inactivation by DNA methylation might have caused the absence or diminution of P16/INK4a expression as previously reported for various types of cancer cells (5,6).

Cancer cell-specific mitotic catastrophe induced by RecQL1 silencing. RecQL1 helicase is highly up-regulated in rapidly proliferating cancer cells and in other transformed cells (28), suggesting that the RecQL1 helicase is needed for genomic stability in rapidly proliferating cells. In this study, we showed that RecQL1-siRNA killed various HCC cell lines by inducing mitotic catastrophe. However, the normal cell lines, TIG-3 fibroblastic cells and APRE19 epithelial cells (Fig. 4), as well as the WI38 and HUVEC cells were all tolerant to *RecQL1* silencing. By contrast, checkpoint-defective cancer cells were sensitive because they failed to stop the cell cycle in order to correct the DNA damage caused by the absence of RecQL1. Notably, P21/WAF1, which is generally induced by TP53 and is important for cell cycle arrest, decreased in many of the HCC cells. Retrovirus integration into host chromosomes and computational simulations have shown that a single double-strand DNA break formed during replication is sufficient to kill cells deficient in DNA repair (29). In cancer cells, mitotic catastrophe due to DNA damage is most probably avoided by highly up-regulated repair enzymes such as RecQL1 that coordinate well with DNA replication to repair DNA damage. HCC cell death caused by silencing the RecQL1 helicase is thus consistent with the findings of Daniel *et al* (29).

Anticancer activity of RecQL1-siRNA in vivo in an orthotopic model of HCC xenograft in mice. The *in vitro* experiment showed that specific cancer cell death can be achieved efficiently by RecQL1 silencing (Fig. 5). RecQL1-siRNA mixed with liver-prone LIC-101 liposomes showed excellent anti-hepatic cancer activity in a mouse orthotopic hepatoma

model (Fig. 5). This anticancer activity was dependent on several cell conditions related to each other as special features of cancer cells: i) high expression of the RecQL1 helicase, ii) active replication of cells, and iii) an impaired checkpoint function that permits cells with DNA damage to enter the M phase. Normal hepatic cells do not have these features and thus they do not show mitotic catastrophe caused by RecQL1 silencing. We propose the systemic administration of the RecQL1-siRNA/LIC-101 complex as an effective therapeutic system against hepatic cancer due to the expected absence of patient drug-associated adverse effects.

Acknowledgements

We thank Ms. Chie Ito for the technical assistance and Professor Masamichi Kojiro of Kurume University School of Medicine for the discussion and encouragement. We also thank Professor Shigeki Arii and Dr Arihiro Aihara of the Tokyo Medical and Dental University for the helpful discussions.

References

1. Llovet JM and Bruix J: Molecular targeted therapies in hepatocellular carcionoma. Hepatology 48: 1312-1327, 2008.
2. Ozturk M: Genetic aspects of hepatocellular carcinogenesis. Semin Liver Dis 19: 235-242, 1999.
3. Elmore LW, Hancock AR, Chang SF, *et al*: Hepatitis B virus X protein and p53 tumor suppressor interactions in the modulation of apoptosis. Proc Natl Acad Sci USA 94: 14707-14712, 1997.
4. Greenblatt MS, Feitelson MA, Zhu M, *et al*: Integrity of p53 in hepatitis B X antigen-positive and -negative hepatocellular carcinomas. Cancer Res 57: 426-432, 1997.
5. Chaubert P, Gayer R, Zimmermann A, *et al*: Germ-line mutations of the p16INK4 (MTS1) gene occur in a subset of patients with hepatocellular carcinoma. Hepatology 25: 1376-1381, 1997.
6. Hui AM, Sakamoto M, Kanai Y, *et al*: Inactivation of p16INK4 in hepatocellular carcinoma. Hepatology 24: 575-579, 1996.
7. Furutani M, Arii S, Tanaka S, *et al*: Decreased expression and rare somatic mutation of the CIP1/WAF1 gene in human hepatocellular carcinoma. Cancer Lett 111: 191-197, 1997.
8. Hui AM, Kanai Y, Sakamoto M, Tsuda H and Hirohashi S: Reduced p21WAF1/CIP1 expression and p53 mutation in hepatocellular carcinomas. Hepatology 25: 575-579, 1997.
9. Kuroki T, Fujiwara Y, Nakamori S, Imaoka S, Kanematsu T and Nakamura Y: Evidence for the presence of two tumor-suppressor genes for hepatocellular carcinoma on chromosome 13q. Br J Cancer 72: 383-385, 1995.
10. Zhang X, Xu HJ, Murakami Y, *et al*: Deletions of chromosome 13q, mutations in retinoblastoma 1, and retinoblastoma protein state in human hepatocellular carcinoma. Cancer Res 54: 4177-4182, 1994.
11. LeRoy G, Carroll R, Kyin S, Seki M and Cole MD: Identification of RecQL1 as a Holliday junction processing enzyme in human cell lines. Nucleic Acids Res 33: 6251-6257, 2005.
12. Sharma S, Stumpo DJ, Balajee AS, *et al*: RecQL, a member of the RecQ family of DNA helicases, suppresses chromosomal instability. Mol Cell Biol 27: 1784-1794, 2007.
13. Sharma S and Brosh RM Jr: Human RecQ1 is a DNA damage responsive protein required for genotoxic stress resistance and suppression of sister chromatid exchanges. PLoS One 12: e1297, 2007.
14. Futami K, Kumagai E, Makino H, *et al*: Induction of mitotic cell death in cancer cells by small interference RNA suppressing the expression of RecQL1 helicase. Cancer Sci 99: 71-80, 2008.
15. Futami K, Kumagai E, Makino H, *et al*: Anticancer activity of RecQL1 helicase siRNA in mouse xenograft models. Cancer Sci 99: 1227-1236, 2008.
16. Murakami T: Establishment and characterization of human hepatoma cell line (KIM-1). Acta Hepatol Jpn 25: 532-539, 1984.
17. Yano H, Kojiro M and Nakashima T: A new human hepatocellular carcinoma cell line (KYN-1) with a transformation to adenocarcinoma. In Vitro Cell Dev Biol 22: 637-646, 1986.
18. Yano H, Maruiwa M, Murakami T, *et al*: A new human pleomorphic hepatocellular carcinoma cell line, KYN-2. Acta Pathol Jpn 38: 953-966, 1988.
19. Murakami T, Maruiwa M, Fukuda K, Kojiro M, Tanaka M and Tanikawa K: Characterization of a new human hepatoma cell line (KYN-3) derived from the ascites of the hepatoma patient (Abs.). Proc 47th Annual Meeting Jpn J Cancer Res p292, 1988.
20. Yano H, Iemura A, Fukada K, Mizoguchi A, Haramaki M and Kojiro M: Establishment of two distinct human hepatocellular carcinoma cell lines from a single nodule showing clonal differentiation of cancer cells. Hepatology 18: 320-327, 1993.
21. Lu YS, Kashida Y, Kulp SK, *et al*: Efficacy of a novel histone deacetylase inhibitor in murine models of hepatocellular carcinoma. Hepatology 46: 1119-1130, 2007.
22. Yano J, Hirabayashi K, Nakagawa S, *et al*: Antitumor activity of small interfering RNA/cationic liposome complex in mouse models of cancer. Clin Cancer Res 10: 7721-7726, 2004.
23. Bressac B, Galvin KM, Liang TJ, Isselbacher KJ, Wands JR and Ozturk M: Abnormal structure and expression of p53 gene in human hepatocellular carcinoma. Proc Natl Acad Sci USA 87: 1973-1977, 1990.
24. Li D, Frazier M, Evans DB, *et al*: Single nucleotide polymorphisms of RecQ1, RAD54L, and ATM genes are associated with reduced survival of pancreatic cancer. J Clin Oncol 24: 1720-1728, 2006.
25. Kitamoto M, Nakanishi T, Kita S, *et al*: The assessment of proliferating cell nuclear antigen immunohistochemical staining in small hepatocellular carcinoma and its relationship to histologic characteristics and prognosis. Cancer 72: 1859-1865, 1993.
26. Adachi E, Hashimoto H and Tsuneyoshi M: Proliferating cell nuclear antigen in hepatocellular carcinoma and small cell liver dysplasia. Cancer 72: 2902-2909, 1993.
27. El-Deiry WS, Harper JW, O'Connor PM, *et al*: WAF1/CIP1 is induced in p53-mediated G1 arrest and apoptosis. Cancer Res 54: 1169-1174, 1994.
28. Kawabe T, Tsuyama N, Kitao S, *et al*: Differential regulation of human RecQ family helicases in cell transformation and cell cycle. Oncogene 19: 4764-4772, 2000.
29. Daniel R, Litwin S, Katz R and Skalka AM: Computational analysis of retrovirus-induced SCID cell death. J Virol 75: 3121-3128, 2001.

Growth inhibitory effects of pegylated IFN-α2b and 5-fluorouracil in combination on renal cell carcinoma cell lines *in vitro* and *in vivo*

FUKUKO MORIYA[1-3], SACHIKO OGASAWARA[1,3], YUJI BASAKI[4], JUN AKIBA[1,3], SAKIKO KOJIRO[1,3], SUGURU FUKAHORI[1,3], HIRONORI ISHIZAKI[1-3], NAOYO NISHIDA[1,3], KEI MATSUOKA[2,3], MASAMICHI KOJIRO[1,3], MICHIHIKO KUWANO[3,4] and HIROHISA YANO[1,3]

Departments of [1]Pathology and [2]Urology, Kurume University School of Medicine, [3]Research Center of Innovative Cancer Therapy of the 21st Century COE Program for Medical Science, Kurume University, 67 Asahi-machi, Kurume, Fukuoka 830-0011; [4]Station-II for Collaborative Research Center, Kyushu University, 3-1-1 Maidashi, Higashi-ku, Fukuoka, Fukuoka 812-8582, Japan

Received May 16, 2008; Accepted July 18, 2008

DOI: 10.3892/ijo_00000050

Abstract. We investigated the effects of pegylated IFN-α2b (PEG-IFN-α2b) alone and PEG-IFN-α2b plus 5-fluorouracil (5-FU) *in vitro* on the proliferation of renal cell carcinoma (RCC) cell lines. After the transplantation of RCC cells into nude mice, we administered IFN (PEG-IFN-α2b or IFN-α2b) alone, 5-FU alone, or IFN (PEG-IFN-α2b or IFN-α2b) plus 5-FU; and investigated tumor volume, tumor weight, the numbers of apoptotic cells and artery-like blood vessels, relative mRNA expression levels of enzymes which relate to 5-FU metabolism, angiogenesis factor, and type I interferon receptor. RCC cells *in vitro* were generally and relatively resistant to the anti-proliferative effects of PEG-IFN-α2b, but the addition of 5-FU augmented IFN-induced anti-proliferative effects with the induction of apoptosis. PEG-IFN-α2b *in vivo* presented stronger anti-tumor effects than IFN-α2b, and its combination with 5-FU augmented the effects. The significant anti-tumor effect of the combination treatment was the increase in apoptotic cell number, but there were no significant differences in the suppression of angiogenesis, expression of IFN receptor, and the actions of metabolic enzymes of 5-FU. In conclusion, PEG-IFN-α2b presents stronger anti-tumor effects than non-pegylated IFN, and the effects are augmented in the combination with 5-FU. Our findings suggest the clinical usefulness of PEG-IFN-α2b in the treatment of RCC.

Correspondence to: Dr F. Moriya, Department of Pathology, Kurume University School of Medicine, 67 Asahi-machi, Kurume, Fukuoka 830-0011, Japan
E-mail: moriya_fukuko@kurume-u.ac.jp

Key words: renal cell carcinoma, pegylated interferon-α2b, 5-fluorouracil, combination therapy, apoptosis

Introduction

Renal cell carcinoma (RCC) is highly resistant to conventional chemotherapy. The objective response rate is 6-9% for vinblastine and 5-8% for 5-fluorouracil (5-FU) (1). The response rates of treatment regimens using interleukin-2 are 6-31% (2), and the therapeutic response rates of interferon (IFN)-α are 4-33% in patients with metastatic RCC (3). The response rates of immunochemical therapies that utilize chemotherapeutic agents with IFN-α or interleukin-2 range between 8 and 39% (4). Immunochemical therapy is the best treatment for advanced RCC, but potential synergetic effects of the medicines as well as their mechanisms remain to be elucidated.

Wadler and Wienik (5) for the first time proposed a combination therapy of IFN-α and 5-FU in 1988 in their study using colon cancer cell lines. Later, this combination therapy was applied to various types of human malignancies including RCC and hepatocellular carcinoma (HCC). 5-FU has two major anti-tumor mechanisms: one involves its active metabolite 5-fluoro-2'-deoxyuridine-5'-monophosphate (FdUMP), inhibiting the activity of thymidylate synthase (TS) and consequently DNA synthesis; the other is related to the incorporation of 5-FU metabolite into RNA and DNA, thereby disrupting normal RNA processing and function. The sensitivity of cancer cells to 5-FU is often influenced by the enzymes affecting 5-FU metabolism, including TS, dihydropyrimidine dehydrogenase (DPD), orotate phosphoribosyl transferase (OPRT), thymidine phosphorylase (TP), uridine phosphorylase (UP) and thymidine kinase (TK).

PEG-IFN-α2b, a new interferon, is a covalent conjugate of recombinant IFN-α2b with monomethoxy polyethylene glycol (PEG) in a 1:1 molar ratio that produces a 31,000-Da molecule (6). PEG conjugation increases the size of the molecule, therefore, the absorption of the pegylated molecule is slower, its serum half-life is longer, and its rate of clearance from the plasma is lower than that of the unmodified molecule. PEG-IFN-α2b thereby increases patient exposure

to IFN-α2b and requires less frequent administration (6). Clinical trials in chronic hepatitis C patients have suggested that PEG-IFN-α preparations produce more potent therapeutic effects than IFN-α preparations (6-10). Yano *et al* (11) examined the *in vitro* and *in vivo* anti-tumor effects of PEG- and non-PEG-IFN-α2b on human liver cancer cells, and they reported that the anti-tumor effect of PEG-IFN-α2b was significantly more potent than that of non-PEG-IFN-α2b. In addition, Motzer *et al* (12) conducted a phase I study of PEG-IFN-α2b on advanced renal cancer patients, and reported that partial response was obtained in 5 (19%) patients. Yet, there have been few basic studies evaluating the efficacy of PEG-IFN-α2b on RCC *in vitro* and *in vivo*.

Our current study examined the *in vitro* and *in vivo* anti-tumor effects of PEG-IFN-αb, IFN-α2b, 5-FU, and the combination of one of the two IFNs and 5-FU, on RCC cell lines, using PEG-IFN-α2b concentrations close to the clinical dosage. We also examined the effects of the therapies on apoptotic cells, artery-like blood vessels, the enzymes affecting 5-FU metabolism, vascular endothelial growth factor (VEGF), and type I IFN receptor subunits in human RCC tumors which were developed in nude mice.

Materials and methods

Cell lines and cell culture. This study used 8 human RCC cell lines. KRC/Y (13) was established in our laboratory. KUR11 and KURM were donated by Professor K. Itoh of the Department of Immunology at our University. Caki-1, Caki-2, and ACHN were purchased from American Type Culture Collection. VMRC-RCW was purchased from Japan Health Sciences Foundation. OS-RC-2 was purchased from Riken Cell Bank (Tsukuba, Japan).

Culture medium for KRC/Y consisted of Dulbecco's modified Eagle's medium (Nissui Seiyaku Co., Tokyo, Japan) supplemented with heat-inactivated (56°C, 30 min) 5% fetal bovine serum (FBS, Bioserum, Vic, Australia), 100 U/ml penicillin and 100 μg/ml streptomycin (Gibco BRL/Life Technologies Inc., Gaithersburg, MD). Culture medium for Caki-1, Caki-2, VMRC-RCW and ACHN consisted of modified Eagle's medium (Gibco); the medium for KUR11, KURM and OS-RC-2 consisted of RPMI-1640; and each medium was supplemented with 10% FBS, 100 U/ml penicillin and 100 μg/ml streptomycin. Cells were cultured in an atmosphere of 5% CO_2 in air at 37°C. 5-FU was purchased from Kyowa Hakko K.K. (Tokyo, Japan).

IFN and reagents. PEG-IFN-α2b (PEG Intron®) and IFN-α2b (Intron® A) were provided by Schering-Plough K.K. (Osaka, Japan). The specific activity of PEG-IFN-α2b was $6.4x10^7$ IU/mg protein and that of IFN-α2b was $2.6x10^8$ IU/mg protein.

Rat antibody against mouse endothelial cells (anti-CD34, clone MEC14.7) was purchased from Serotec Co., Oxford, UK; and mouse monoclonal antibody against human α-smooth muscle actin (SMA) that cross-reacts with mouse α-SMA (clone 1A4), from Immunon (Pittsburgh, PA).

Effects of PEG-IFN-α2b on the proliferation of RCC cell lines in vitro. The effects of PEG-IFN-α2b or 5-FU on cell proliferation were examined in colorimetric assays by using 3-(4,5-dimethylthiazol-2yl-yl-)-2,5-diphenyl tetrazolium bromide (MTT) cell growth assay kits (Chemicon International Inc.) as described elsewhere (14). Briefly, the RCC cells ($1.5\text{-}5x10^3$ cells per well) were seeded on 96-well plates (Nunc Inc., Roskilde, Denmark), cultured for 24 h, and the culture medium was changed to a new medium with or without PEG-IFN-α2b (8, 32, 128, 512 or 2,048 IU/ml). After culturing for 24, 48, 72 or 96 h, the number of viable cells was measured with ImmunoMini NJ-2300 (Nalge Nunc International, Tokyo, Japan) by setting the test wavelength to 570 nm and the reference wavelength to 630 nm. To keep the optical density within linear range, all experiments were performed when the cells were in the logarithmic growth phase. The effects of IFN-α2b on the growth of VMRC-RCW cells were also examined in the same manner.

Effects of combination therapy of PEG-IFN-α2b and 5-FU on the proliferation of RCC cell lines in vitro. RCC cells (VMRC-RCW, 3,000 cells/well) were seeded on 96-well plates (Nunc Inc.), cultured for 24 h, and then the culture medium was changed to a new medium containing PEG-IFN-α2b alone (0, 160, 317, 625, 1,250, 2,500, 5,000 or 10,000 IU/ml); 5-FU alone (0, 0.6, 1.25, 2.5, 5 or 10 μM); or both 5-FU (0, 0.6, 1.25, 2.5, 5, 10 μM) and PEG-IFN-α2b (0, 160, 317, 625, 1,250, 2,500, 5,000 or 10,000 IU/ml). After 96 h of culture, the number of viable cells was examined by MTT assay as described above.

The synergy of cooperative cytotoxicity was determined by the median-effect principle as described by Chou and Talalay (15). Data from each sample were analyzed by using CalcuSyn ver. 2 (Biosoft, Cambridge, UK).

Morphological observation. For morphological observation by light microscopy, 8 RCC cell lines were seeded on Lab-Tek tissue culture chamber slides (Nunc Inc.), cultured with or without PEG-IFN-α2b (1,024, 4,098 or 8,192 IU/ml) for 72 h, fixed for 30 min in Carnoy's solution, and stained with hematoxylin and eosin (H&E).

In another experiment, one RCC cell line (VMRC-RCW, 8,000 cells/chamber) was seeded on Lab-Tek tissue culture chamber slides (Nunc Inc.), cultured with PEG-IFN-α2b alone (0, 160, 317, 625, 1,250, 2,500, 5,000 IU/ml); 5-FU alone (0, 0.6, 1.25, 2.5, 5.0 μM); PEG-IFN-α2b (0, 160, 317, 625, 1,250, 2,500, 5,000 IU/ml) plus 5-FU (0, 0.6, 1.25, 2.5, 5.0 μM), or PBS, for 72 h, fixed for 30 min in Carnoy's solution and H&E stained.

Effects of PEG-IFN-α2b and IFN-α2b on RCC cell proliferation in nude mice. Cultured VMRC-RCW cells ($1.0x10^7$ cells/mouse) were subcutaneously (s.c.) injected into the backs of 4-week-old female BALB/c athymic nude mice (n=62) (Clea Japan, Inc, Osaka, Japan). One week later when the largest diameter of the tumor reached ~10 mm (day 0), the mice were divided into 7 groups (n=8 or 9 each) in a manner to equalize the mean tumor diameter of each group. Each mouse received a subcutaneous injection of 0.1 ml of medium alone (control group), medium containing 640, 6,400, 64,000 or 640,000 IU of PEG-IFN-α2b, or medium containing 640 or 6,400 IU of IFN-α2b, twice a week for 2 consecutive weeks (on day 1, 4,